trapping of the photoexcited electron on a localized Si dangling bond in the band gap (*17*). However, these data are consistent with simple models of carrier escape by tunneling, as proposed by Vial *et al.* for PS (*9*). Our observation of similar lifetimes in isolated nanocrystals and in aggregates reveals that tunneling to larger crystallites does not control the dynamics. Surface silanol groups and adsorbed water may affect the dynamics, because, the luminescence of both nanocrystals (*12*) and PS (*19*) is strong at acid pH and quenched at neutral and basic pH.

REFERENCES AND NOTES

1. Recent reviews: A. Henglein, *Chem. Rev.* **89**, 1861 (1989); Y. Wang and N. Herron, *J. Phys. Chem.* **95**, 525 (1991); H. Weller, *Angew. Chem. Int. Ed. Engl.* **105**, 41 (1993); L. Brus, *Appl. Phys. A* **53**, 465 (1991).
2. However, for studies of indirect AgBr, see K. P. Johansson, A. P. Marchetti, G. B. McLendon, *J. Phys. Chem.* **96**, 2873 (1992) and U. Scholle, H. Stolz, W. von der Osten, *Solid State Commun.* **86**, 657 (1993).
3. J. P. Proot, C. Delerue, G. Allan, *Appl. Phys. Lett.* **61**, 1948 (1992).
4. T. Takagahara and K. Takeda, *Phys. Rev. B* **46**, 15578 (1992).
5. M. S. Hybertsen, *Mater. Res. Soc. Symp. Proc.* **256**, 179 (1992).
6. V. Petrova-Koch *et al.*, *J. Appl. Phys.* **61**, 943 (1992).
7. L. T. Canham, *Appl. Phys. Lett.* **57**, 1046 (1990).
8. V. Lehmann and U. Gosele, *ibid.* **58**, 856 (1991).
9. J. C. Vial *et al.*, *Phys. Rev.* **45**, 14171 (1992).
10. H. Koyama, M. Araki, Y. Yamamoto, N. Koshida, *Jpn. J. Appl. Phys.* **30**, 3606 (1991).
11. Y. H. Xie *et al.*, *J. Appl. Phys.* **71**, 2403 (1992).
12. K. A. Littau, P. F. Szajowski, A. J. Muller, A. R. Kortan, L. E. Brus, *J. Phys. Chem.* **97**, 1224 (1993). The first stage of the aerosol apparatus now operates at 1000°C. The second, chemical oxidation step is now carried out by the heating (110°C, 1 hour) of the colloid after the addition of water (pH 0.8, 5% by volume) and 30% hydrogen peroxide (9% by volume).
13. C. B. Murray, D. J. Norris, M. G. Bawendi, *J. Am. Chem. Soc.* **115**, 8706 (1993).
14. As described in (*12*), QY measurements are made by direct comparison with dye luminescence.
15. Equation 2 of R. Rossetti, J. L. Ellison, J. M. Gibson, and L. E. Brus [*J. Chem. Phys.* **80**, 4464 (1984)]. The Si dielectric data are from D. E. Aspnes and A. A. Sunda [*Phys. Rev. B* **27**, 985 (1983)].
16. At higher resolution, the excitation spectrum might show TO phonon structure.
17. A numerical calculation of Si nanocrystal spectra shows a somewhat similar, indirect gap–like spectrum (G. Delerue, G. Allan, M. Lannoo, unpublished data.
18. P. D. J. Calcott, K. J. Nash, L. T. Canham, M. J. Kane, D. Brumhead, *J. Phys. Condens. Matter* **5**, L91 (1993).
19. J. K. M. Chun, A. B. Bocarsly, T. R. Cottrell, J. B. Benzinger, J. C. Yee, *J. Am. Chem. Soc.* **115**, 3024 (1993).

29 June 1993; accepted 23 September 1993

Real-Time Observation of the Vibration of a Single Adsorbed Molecule

Fumiya Watanabe, Gary M. McClelland,* Harry Heinzelmann†

The newly developed femtosecond field emission camera was used to observe the time dependence of field emission through a single copper phthalocyanine molecule adsorbed on a tungsten tip. In many of the individual 212-picosecond-long recordings, the field emission was found to oscillate with a frequency between 5 × 10^{10} and 20 × 10^{10} hertz. The oscillations, which were not observed from a bare tip, are believed to arise from the vibration of a single molecule with respect to the surface. Numerical simulations confirmed the statistical significance of the data.

For the investigation of the atomic and molecular motions that govern chemical and physical processes, the ideal measurement would observe continuously a single molecule or collision on the time scale of atomic motion. Such a measurement would, however, require both the sensitivity to observe a single molecule without strongly perturbing its motion and a time resolution on the time scale of a molecular vibration, between 10^{-14} and 10^{-11} s. Although single atoms and molecules may now be routinely imaged, the fast laser techniques used for probing molecular dynamics (*1*) are, generally, too insensitive for the observation of individual molecules. Repeated pumping techniques may be used, however (*2*). Because optical transitions strongly perturb a molecule by changing its electronic state, laser methods cannot give continuous measurements on a single molecule. These problems can be overcome by the femtosecond field emission camera (FFEC) (*3, 4*), an instrument we have developed to continuously record the motion of individual atoms and molecules with a temporal resolution as fast as 10^{-14} s. Here, we report the continuous observation of the dynamics of a single molecule, with the recording of the vibrational motion of single copper phthalocyanine (CuPc) molecules adsorbed on a tungsten tip.

In a strong electric field, the width of the potential barrier that normally traps electrons in a metal can be reduced sufficiently to allow field emission (FE), the quantum mechanical tunneling of electrons into vacuum (Fig. 1). In the FFEC, FE is induced by the application of ≈ -1000 V to a metal tip, which concentrates the electric field (F) at the tip surface to ≈ 1 V Å^{-1} (*3*). If the tip is very sharp, the FE can be confined to a subnanometer high-field region at the apex and may be as large as 10^{-5} A (*5*) or 10^{14} e^- s^{-1}. Thus, many electrons will be emitted during the vibrational period of heavier atoms and molecules that may be present on the surface. The intensity of the FE depends strongly on the position of any adsorbates, which change the barrier height and contribute localized electronic states. Thus, a molecular vibrational motion on the tip will cause an FE oscillation, which we resolve by focusing the emitted electrons into a beam that is electrostatically swept across an efficient detector (Fig. 2). The spatial variation of the detected electron intensity records the temporal variation of the FE. Because the metal tip is an ideal point source for focusing and the time-of-flight spread of the electrons in the strong tip field is very small, a resolution of 10^{-14} s is achievable (*3*). Unlike laser techniques, the FFEC is limited to observing dynamics on sharp tips.

For our initial study of single-molecule dynamics, we chose the vibration of a large rigid molecule, CuPc (Fig. 3A), expecting that its large mass and vibrational amplitude would give a slow vibration with respect to the surface. The components of the electric polarizability of CuPc parallel ($\alpha_\parallel$) and perpendicular ($\alpha_\perp$) to the molecular plane are ≈ 100 and ≈ 45 Å^3 (*6*), respectively. In a strong field (F), the polarization potential for the molecule's pivoting down by an angle θ (Fig. 3B) from perpendicular toward parallel to the surface is $\frac{1}{2}F^2(\alpha_\parallel - \alpha_\perp)\sin^2\theta$, which at $F = 1$ V Å^{-1} favors, by 2 eV, the perpendicular over the parallel orientation. For this pivoting motion, the moment of inertia (I_L) is ≈ 5600 atomic mass units·Å^2, giving a vibrational frequency of 15 × 10^{10} Hz. If this vibration were excited to an energy of kT (where T is the temperature and k is the Boltzmann constant), at T = 1000 K the end of the molecule would move 7 Å, large enough to give a sizable change in the FE. The field-free adsorption potential of the molecule would ordinarily favor θ near $\pi/2$, which counteracts the polarizability potential and thereby reduces the frequency. These estimates show that of the many vibrational modes, at least one should be resolvable within our present 1- to 2-ps resolution. Other adsorption geometries might have

---

IBM Research Division, Almaden Research Center, San Jose, CA 95120.

---

*To whom correspondence should be addressed.
†Present address: Institute of Physics, University of Basel, 4056 Basel, Switzerland.

vibrational frequencies equally as low.

Adsorption of a single CuPc molecule can enhance the FE by 100-fold or more (7). The mechanism probably involves tunneling into the adsorbed molecule and then out into a field enhanced by the "sharp" molecular shape (8, 9). Bistable (10 ms) variations of the FE that are a result of the flopping of individual CuPc molecules between local potential minima have been observed previously (7). CuPc is a very stable molecule, thermally decomposing only above 1100 K (10).

Neon sputtering and thermal annealing are used to sharpen a tungsten tip oriented along the ⟨111⟩ axis to an apex ≈2 nm across (5). To image the tip by FE microscopy, we turned off the electrostatic lens and held the tip at ≈ −500 V to project an unfocused, low FE current of 10^{-11} A onto the screen (3). The CuPc was then sublimated slowly onto a tip cooled to 80 K, so that at ≈100-s intervals a molecule arrived near the apex, which caused an abrupt change in the FE. The first few molecules reduced the FE, probably by chemisorbing or decomposing on the surface to form an overlayer that increases the FE barrier height or width (8). There was eventually an abrupt increase (a factor ≥50) in the local emission, which indicates that the FE is controlled by a single molecule on the tip. Presumably, a molecule is physisorbed to the overlayer. Deposition was at this point stopped. In the time-resolved experiments, the deflecting field was ramped to sweep the beam while we increased the FE to 10^{-5} A by pulsing the tip to approximately −1000 V for ≈2 ns. During the sweep, the molecule may be excited by the changing field at the tip (8, 9) or by FE-induced heating. After each sweep, the low-current FE image was observed to check that the molecule was still emitting. However, within 20 sweeps after the original increase in brightness, the FE image intensity decreased, presumably because during the sweep the molecule decomposed or diffused off the end of the tip. Deposition was then restarted until another bright spot appeared and more sweeps were performed. To maximize the chance of observing single molecule dynamics, for each increase in brightness we analyzed only the three proceeding sweeps. A total of 270 sweeps were analyzed.

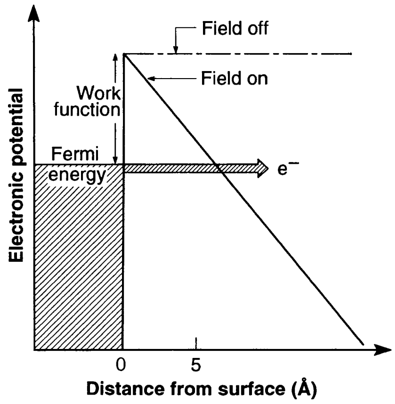

Fig. 1. Potential energy diagram for electrons near a tungsten surface. In a large field, the barrier width is reduced, allowing the tunneling process called field emission. The motion of an adsorbed atom or molecule alters the barrier region, which changes the emission.

Even if the FE always occurs through a molecule bound to the surface by a low-frequency vibrational mode, the vibration will often not be sufficiently excited to be observed above the shot noise. Also, because the vibrational frequency of such a large molecule is likely to change between sweeps as the molecule changes its surface position, averaging over many traces will obscure the vibration. Thus, we searched for periodic behavior in entire individual traces and portions of traces as described below. Although the periodicity can often be seen directly in a plot of $S_t(t)$, the time dependence of the FE, and is quite clear in the autocorrelation function $C_t(t)$ (11), each trace was Fourier-transformed (12) and normalized to generate a plot of the power spectrum, $M_t(\nu)$, versus frequency between 5×10^{10} and 20×10^{10} Hz. These spectra were used to test the statistical significance of the data, which were obtained on six separate days over a period of 6 months.

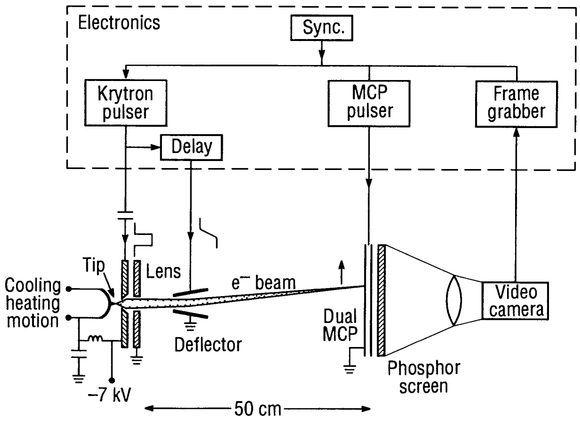

Fig. 2. The femtosecond field emission camera is shown here not to scale; the tip-lens distance is 0.7 cm. Field emission is temporally resolved by sweeping the electron beam across the screen. MCP, microchannel plate; Sync., synchronizing pulse.

Six traces recorded a sharp step change in the FE. Because only a 212-ps section of each 2-ns-long FE pulse was recorded, many more such changes undoubtedly went unobserved. Abrupt changes in the FE probably correspond to large changes in the position of a CuPc molecule, which should often result in vibrational excitation. To search for such excitation, we looked for a peak in the normalized power spectrum $M_t(\nu)$, computed from the measured FE between the initial abrupt change and the end of the trace. Of the six traces, three clearly showed sharp spectral peaks in $M_i(\nu)$, each at a different frequency (6.5×10^{10}, 8.1×10^{10}, and 12.2×10^{10} Hz). The example shown in Fig. 4A shows a modulation at 6.5×10^{10} Hz, with a peak-to-peak sinusoidal variation equivalent to 48% of the average intensity. In all traces, the intensity was decreased at early and late times, when the e⁻ beam was partially occluded by the deflecting plates.

Even in the absence of sudden changes in molecular position, the vibrational energy of the CuPc molecule can be increased gradually by the FE process itself. The Nottingham effect (13) heats the electrons in the tip, which can then transfer energy to the molecular vibrations, or tunneling electrons can directly excite a CuPc vibration (14). Figure 4B shows a trace that does not contain an abrupt change but shows a distinct peak in $M_t(\nu)$. The peak-to-peak sinusoidal variation at 9.3×10^{10} Hz is 46% of the average FE. In 6 of the 267 full traces, a peak in the normalized power spectrum appeared that was ≥8.7 times the

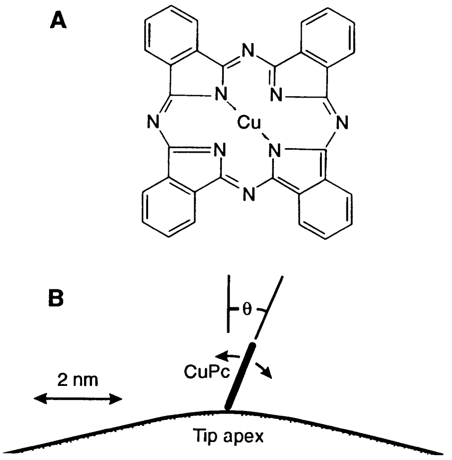

Fig. 3. (**A**) The CuPc molecule. (**B**) Schematic of a CuPc molecule (viewed edgewise) adsorbed on the end of a tungsten tip, showing a possible observed vibrational motion. The perpendicular orientation is energetically favored by high electric fields.

frequency-averaged power. These peaks occurred at frequencies (of 10^{10} Hz) of 5.1, 7.0, 8.4, 9.3, 17.7, and 18.6.

Because a low-frequency molecular vibration is likely to be strongly coupled to other slow motions, the large-amplitude vibration may occur continuously for only several vibrational periods at a time. Hence, we computed the frequency power spectra for 123-ps-long sections of the traces that were situated at the beginning, middle, and end of each trace. Of the 801 sections analyzed at the beginning, middle, and end of each trace (3 × 267 total), 5 showed peaks with intensities ≥8.5 times the average power, at frequencies (of 10^{10} Hz) of 5.1, 11.2, 13.0, 18.6, and 20.0. The two traces that had sections peaking at 5.1 × 10^{10} and 18.6 × 10^{10} Hz also showed prominent peaks, as noted above, in the full-length traces. The example in Fig. 4C shows a sinusoidal signal variation (at 5.1 × 10^{10} Hz) of 66% of the average intensity, which is a factor of 2.0 variation.

To establish that the spectra containing large peaks were not simply ones in which the random noise happened to peak at a particular frequency, we extensively modeled the statistical properties of the noise. For each set of model parameters, $M_i(\nu)$ was computed for each of ≈10,000 simulated noise traces. In addition to having the correct overall shape (usually a bell curve), each trace included the shot noise, the exponential gain statistics of the microchannel plate detector, and the measured optical slit function. To model the possibility that an adsorbate moving randomly on the tip might by chance mimic a periodic motion over the limited duration of the trace, we included a random flip-flop signal, which varied between two discrete values with Poisson statistics. The results of the simulation were expressed as the probability distribution of the maximum peak height in the $M_i(\nu)$. Largely because the values for $M_i(\nu)$ (experimental as well as simulated) are normalized by the average frequency spectra, this distribution is quite insensitive to the model's parameters. The results of the simulation were affected only slightly, for example, by omission of the exponential gain statistics, by a change of the bell curve to a constant, or by omission of the flip-flop component. Obtaining a factor of 2 change in the relevant probability required an unrealistic change in the model.

From the simulations, without a periodic oscillation only 1 of every 500 full traces is expected to show a peak >8.70 in $M_i(\nu)$, whereas experimentally 6 out of 267 traces (Fig. 4B) showed such peaks. Similarly, for the 123-ps-long sections of the traces, only about 1 in 4000 noise traces is expected to peak at >8.5, whereas 5 such traces (Fig. 4C) were observed experimentally out of 801. For example, the probability that a particular section should have an oscillation with the amplitude seen at the end of Fig. 4C is 2 × 10^{-6}. Finally, the probability of any three of six noise spectra being as peaked as the three we observed after an abrupt FE change is 0.03. As a control, 100 traces were analyzed from a clean tungsten tip with no adsorbates. No large peaks were observed, and the statistics agreed with the predictions of our model noise calculations. Our simulations thus confirm that the observed frequency peaks are caused by periodic motion on the tungsten tip, not by random noise or by random motion.

It is possible, however, that we observed not the vibration of single CuPc molecules but rather the vibration of molecular fragments or clumps of molecules. The fact that the FE showed a sudden factor of 50 increase during a very slow deposition is strong evidence that almost all of the detected FE was from a single molecule. The 13 observed vibrational frequencies are rather evenly distributed within the experimentally accessible 5 × 10^{10} to 20 × 10^{10} Hz range. This distribution could arise from the occupation of different molecular binding sites or orientations, the varying position of surrounding molecules or fragments, or varying local field strengths at different parts of the tip. The vibrational frequency is expected to change between sweeps as the molecule occupies new local potential minima in the changing electric field. It seems unlikely that the observed oscillations arose from a changing of the effective FE potential by repeated electronic charging and discharging of a nanometer-size particle on the tip, as so few electrons would be needed for charging that the process would not be periodic but irregular, dominated by the statistics of individual e^- events.

The ability to observe single atomic and molecular events in real time opens up entirely new possibilities in molecular dynamics. It allows observation of spontaneous processes that cannot be optically synchronized and observed in pump-probe experiments. As shown elsewhere, experiments can be performed on tips that have been atomically imaged by field ion microscopy (*3*). With the use of astigmatic e^- focusing, the FE can be simultaneously dispersed both spatially and temporally to obtain a moving picture (*3*). Observing real-time dynamics will contribute to the ability to precisely control individual atoms and to use them in electronic and mechanical devices (*15*).

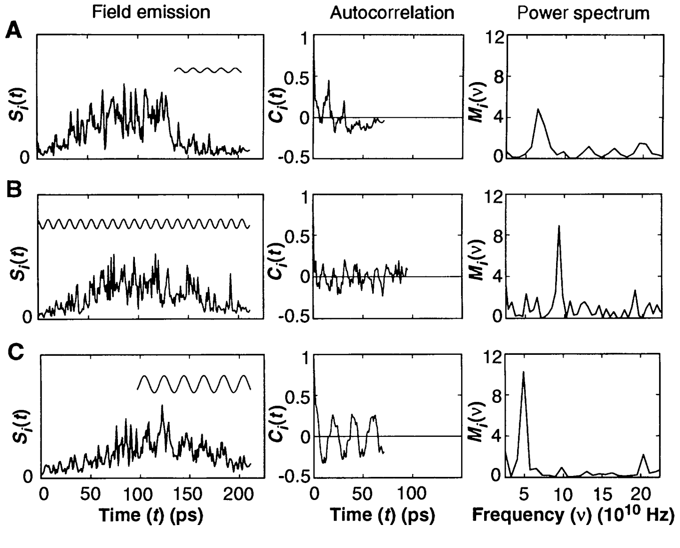

Fig. 4. Three individual time records showing sinusoidal FE oscillations attributed to molecular vibration. The first column plots the FE [$S_i(t)$] (during the i^{th} sweep) versus time. Over the time interval in which a sinusoidal oscillation was detected, the smooth sinusoid above the data represents the amplitude of the observed oscillation with the noise removed. The second and third columns present the autocorrelation function [$C_i(t)$] (*11*) and the power spectrum [$M_i(\nu)$] (*12*), respectively. In (**A**), an oscillation is observed after an abrupt change in FE; in (**B**), the oscillation continues through most of the trace; and in (**C**), the oscillation occurs during the last half of the trace.

REFERENCES AND NOTES

1. M. Dantus, H. H. M. Janssen, A. H. Zewail, *Chem. Phys. Lett.* **181**, 281 (1991); L. Khundkar and A. H. Zewail, *Annu. Rev. Phys. Chem.* **41**, 15 (1990); R. R. Cavanagh, D. S. King, J. C. Stephenson, T. F. Heinz, *J. Phys. Chem.* **97**, 786 (1993).
2. R. J. Hamers and D. G. Cahill, *J. Vac. Sci. Technol. B* **9**, 514 (1991).
3. H. Heinzelmann, F. Watanabe, G. M. McClelland, *Phys. Rev. Lett.* **70**, 3611 (1993).
4. G. M. McClelland, U.S. patent 5151594 (1992).
5. H -W. Fink, *IBM J. Res. Dev.* **30**, 460 (1986); *Phys. Scr.* **38**, 260 (1988).
6. M. A. Barrett, Z. Borkowska, M. W. Humphreys, R. Parsons, *Thin Solid Films* **28**, 289 (1975).
7. Ch Kleint and K. Mockel, *Surf. Sci.* **40**, 343 (1973); W. Schutt, H. Koster, G. Zuther, *ibid.* **45**, 163 (1974).
8. A. J Melmed and W. W Muller, *J. Chem. Phys.* **29**, 1037 (1958).
9. R. Gomer and D. A. Speer, *ibid.* **21**, 73 (1953).
10. E. A. Lawton, *J. Phys. Chem.* **62**, 384 (1958).
11. The FE intensity for the i^{th} sweep was recorded as a series $S_i(nt_0)$ of FE strengths at times $t = nt_0$ separated by $t_0 = 9.6 \times 10^{-13}$ s. The autocorrelation function was computed by $C_i(mt_0) = \Sigma_n S_i(nt_0) S_i[(n + m)t_0]$, where $S_i(nt_0)$ is

obtained by subtracting from $S_i(nt_0)$ a smooth fit to $S_i(nt_0)$ and normalizing.

12. The power spectrum for the i^{th} sweep,

$$P_i(\nu) = |\Sigma_n \exp(i2\pi\nu nt_0)S_i(nt_0)|^2$$

was computed for frequencies between 5×10^{10} and 20×10^{10} Hz. Frequencies below this range were dominated by the overall trace shape, whereas those above require too good a beam focus to observe a signal. Each spectrum was normalized by its frequency average to form $I_i(\nu) = P_i(\nu)/\langle P_i(\nu)\rangle_\nu$. After $I_i(\nu)$ was computed for a series of sweeps, an average normalized power spectrum was computed, and this was used to calculate $M_i(\nu) = I_i(\nu)/\langle I_i(\nu)\rangle_i$, the individual sweep power spectrum normalized by the average power spectrum.

13. H. Bergeret, A. Septier, M. Drechsler, *Phys. Rev. B* 31, 149 (1985).
14. E. L. Wolf, *Principles of Electron Tunneling Spectroscopy* (Oxford Univ. Press, New York, 1985); V. T. Binh, S. T. Purcell, G. Gardet, N. García, *Surf. Sci.* **279**, L197 (1992).
15. D. M. Eigler and E. K. Schweizer, *Nature* **344**, 524 (1990); D. M. Eigler, C. P. Lutz, W. E. Rudge, *ibid.* **352**, 600 (1991).
16. This work was partially supported by the Office of Naval Research contract N00014-88-C-0419 and the Air Force Office of Scientific Research contract F49620-89-C-0068. H.H. thanks the Swiss National Science Foundation and the Treubelfonds, Basel, Switzerland, for fellowships.

16 July 1993; accepted 24 September 1993

Effective Coupling in Biological Electron Transfer: Exponential or Complex Distance Dependence?

Jeffrey W. Evenson and Martin Karplus*

Calculations for a simple model electron transfer system and tuna cytochrome c demonstrate a dichotomy in the distance dependence of the effective coupling. In one regime, the effective coupling varies exponentially with distance and depends primarily on the average properties of the bridging material; in the other regime, the effective coupling has a complex distance dependence and is more sensitive to the details of the bridging material. Experiments and theory indicate that both regimes may occur in biological systems, providing a perspective on a recent controversy over the nature of the distance dependence.

Electron transfer is fundamental to a wide range of important biological processes, including respiration and photosynthesis (*1*). Recent experimental advances, such as structural data for relevant proteins (*2*), provide a basis for meaningful theoretical approaches to the transfer rate. From analysis of biological electron transfer systems and model proteins, a controversy has arisen concerning the dependence of the electronic coupling on the distance between the donor and the acceptor (*3*). It has been suggested both that there is a universal exponential dependence on the distance (*4*) and that the distance dependence is a complex function of the intervening material (*5*). These suggestions are not mutually exclusive. Depending on the energy difference between the bridge orbitals and the donor-acceptor orbitals, the electronic coupling can vary exponentially with distance or have a more complex behavior. The present treatment is based on the inverse matrix technique (*6*) for calculating the electronic coupling that includes all paths between the donor and acceptor. We apply the approach first to a one-dimensional (1D) (single-pathway) model and then to a calculation including all possible pathways between the heme and arbitrarily located acceptors in tuna cytochrome c (*7*).

The rate k for the long-distance, nonadiabatic electron transfer reactions occurring in proteins is usually assumed to be given by (*8*)

$$k = \frac{2\pi}{\hbar} |H_{\mathrm{DA}}|^2(\mathrm{F.C.}) \qquad (1)$$

where $\hbar$ is Planck's constant divided by 2π. Electronic degrees of freedom determine the effective coupling (H_{DA}), and nuclear degrees of freedom determine the Franck-Condon factor (F.C.). The effective coupling is explicitly dependent on the tunneling energy E (*6*), as is clear from the definition for H_{DA} in the one-electron approximation (*9*), which is given by

$$H_{\mathrm{DA}} = -\sum_{ij} \beta_{\mathrm{D}i} G_{ij}(E) \beta_{j\mathrm{A}} \qquad (2)$$

Here, $G(E) = (H_{\mathrm{bridge}} - E)^{-1}$ is the Green's function (*10*) for the bridge Hamiltonian H_{bridge}. The indices i and j run over all orbitals involved in the transfer process, and $\beta_{\mathrm{D}i}$ ($\beta_{i\mathrm{A}}$) represents the coupling of the ith orbital to the donor (acceptor). Widely used pathway models approximate Eq. 2 by calculating the Green's function to lowest order in perturbation theory (*10*). In the single-pathway model, only the term that makes the most significant contribution to the sum is retained. The inverse matrix technique is an alternative to the approximate pathway method (*6*). It exploits the ease of matrix inversion to compute the Green's function exactly, including all terms in the sum. Although the pathway method may provide qualitative insight, more accurate methods, such as full matrix diagonalization or the more powerful inverse matrix technique (*6*, *11*), are often required to attain quantitative accuracy.

The behavior of the effective coupling H_{DA} is labeled "exponential" if it depends exponentially on the donor-acceptor distance, and "complex" if its distance dependence is not exponential and is sensitive to the material intervening between donor and acceptor. The correlation coefficient $\rho(r, \log H_{\mathrm{DA}})$ between the donor-acceptor distance r and $\log H_{\mathrm{DA}}$ characterizes the behavior (*12*). If the effective coupling is an exponentially decaying function of distance, $\rho = -1$. If ρ is significantly different from -1 (greater than -0.5, say), we label the system as "complex."

An analytically solvable model, which has served as the starting point for many investigations since McConnell's original analysis (*13*), illustrates the classification scheme. The model consists of a donor orbital and an acceptor orbital with tunneling energy E connected to opposite ends of a linear chain of identical bridging ligands (Fig. 1A). We assume one orbital of energy E_{b} per ligand and include only nearest-neighbor coupling with hopping matrix element β. The behavior of the effective coupling is determined by the dimensionless parameter α (*6*)

$$\alpha = \frac{E_{\mathrm{b}} - E}{2\beta} \qquad (3)$$

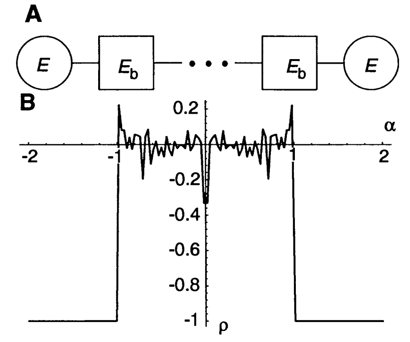

Fig. 1. (**A**) The McConnell model (*13*). Circles represent donor and acceptor orbitals, squares correspond to bridging orbitals, and lines represent coupling between orbitals with hopping matrix element β. The donor and acceptor terminate the chain and have energy E. The bridging orbitals have energy E_{b}. (**B**) Correlation coefficient ρ as a function of the dimensionless parameter α for the model 1D system. For a particular α, ρ is the correlation coefficient for the set $\{(2, \Delta_2), (3, \Delta_3), \ldots, (50, \Delta_{50})\}$, where Δ_n is the logarithm of the effective coupling for a bridge with n links. The effective coupling was computed analytically with a formula derived in (*6*).

Departments of Chemistry and Physics, Harvard University, Cambridge, MA 02138.

*To whom correspondence should be addressed.